

## Ultraviolet (A) and Short-Wave Radiation on the Juneau Icefield, Alaska

By Timothy Quakenbush and Gerd Wendler\*

**Abstract:** Polar ozone depletion has led to interest in ultraviolet light (UV) at the Earth's surface. High resolution spectral measurements were carried out on the Juneau Icefield in Southeast Alaska in the summer of 1991 to study the UV-A (320-400 nm) and short wavelength visible (400-600 nm) radiation field in and above a snow covered area. Radiative measurements of the sun, clear and cloudy sky and the reflectivity and extinction of a glacier snow pack were performed.

Clear sky measurements agree with a Rayleigh scattering atmosphere. Comparing direct solar radiation to diffuse radiation from a cloudy sky indicate clouds scatter evenly across the observed wavelengths with absorption by water drops increasing the extinction in the UV and yellow-red ranges.

The reflectivity of snow was highest in the blue (90 %). It decreased to 78 % at 350 nm, and to 88 % at 600 nm. Its absolute values depend on the physical characteristics of the snow cover.

The extinction coefficient of UV in snow was higher than the mean of the short wavelength band of the visible spectrum. Values ranged from  $10 \text{ m}^{-1}$  at 330 nm, dropped to about  $4 \text{ m}^{-1}$  in the blue (480 nm), and climbed to  $9 \text{ m}^{-1}$  at 590 nm. Larger extinction values occur at longer wavelengths. This final point is probably the most interesting and has been made possible due to a quartz fiber optic light guide. It carries light from inside snow or ice to a spectrometer, making high resolution measurements in these media possible with minimal disturbance to the medium itself.

**Zusammenfassung:** Die Abnahme des Ozons in Polargegenden hat zu einem erhöhten Interesse an der ultravioletten Strahlung geführt. Spektrale Strahlungsmessungen mit hoher Auflösung wurden im Sommer 1991 auf dem Juneau Icefield, Alaska, ausgeführt. Diese Messungen wurden für direkte Sonnenstrahlung, diffuse Strahlung mit und ohne Wolken, und für die Reflexion und Extinktion der Schneedecke im ultravioletten (A, 320-400 nm) wie im kurzwelligen sichtbaren Bereich (400-600 nm) ausgeführt.

Messungen des wolkenlosen Himmels zeigen eine Rayleigh streuende Atmosphäre. Die diffuse Strahlung unter einer Stratus-Wolkendecke zeigt im Vergleich zur direkten Sonnenstrahlung eine erhöhte Extinktion im ultravioletten wie im gelb-roten Teil des Spektrums.

Die Reflexion des Schnees hat ihren höchsten Wert im blauen Bereich (90 %) und nimmt gegen den ultravioletten Bereich (78 % bei 350 nm) wie gegen längere Wellenlängen (88 % bei 600 nm) ab. Der Absolutwert hängt von den physikalischen Bedingungen des Schnees ab.

Der Extinktionskoeffizient des Schnees war im blauen Bereich am niedrigsten ( $4 \text{ m}^{-1}$  bei 480 nm), und nahm gegen den ultravioletten Bereich ( $10 \text{ m}^{-1}$  bei 330 nm) als auch gegen längere Wellenlängen ( $9 \text{ m}^{-1}$  bei 590 nm) zu. Noch höhere Extinktionswerte werden für größere Wellenlängen gefunden. Dieser letzte Punkt ist wohl der interessanteste; die Messung der Extinktion in der fragilen Schneedecke wurde möglich durch eine Quarz-Faseroptik, die das Licht von dem zu messenden Medium in das Spektrometer führt ohne dieses dabei nennenswert zu stören.

### INTRODUCTION

In the classic paper by FARMAN et al. (1985) a substantial decrease in ozone was observed in Antarctica based on observations by the British Antarctic Survey. Considerable work has been done toward understanding the polar ozone depletion process (CRUTZEN & ARNOLD 1986, BRUNE 1991). The reduction in the amount of stratospheric ozone is most prominent in high southern latitudes during austral spring. However, it also occurs to a lesser degree in the Arctic (BRUNE 1991). During the Arctic spring a large fraction of the polar regions are covered with snow.

Most of the ultra-violet light is absorbed by a small amount of ozone, equivalent to a layer 3-4 mm thick at standard atmospheric pressure. The small change in surface UV radiation could have a large effect on life since it is much more biologically active compared to the visible range of the solar spectrum.

A fair amount of work has been done on the radiative characteristics of snow and ice in the visible wavelength range, however, little has been done for wavelengths shorter than 400 nm. During the summer of 1991 measurements were carried out on the reflectivity, transmittance and absorption of snow and ice on a glacier in southern Alaska. Our measurements were performed in the UV-A and short wavelength end of the spectrum (320-600 nm). The signal to noise ratio of our measurements in the UV-B band (280-320 nm) were too small for the data to be useful, however, the methods described later are applicable in this region which is so important to life processes on Earth. Absorption by ozone is very strong in the UV-B band, and weak in the UV-A band.

Measurement of light extinction in snow has traditionally been difficult to perform. Before the advent of quality fiber optic light guides, the entire measuring instrument or detector was placed in a hole in the snow. This makes for a substantial disturbance of the snow pack. An alternative method was to cut out samples of snow or ice and analyze their absorption characteristics in a cold room, also leaving open the possibility of disturbances. In contrast to these older methods, the measurements presented here were taken *in situ* with a synthetic quartz fiber bundle and an Ebert-Fastie spectrometer. The spectrometer is capable of the very high resolution of  $0.5 \text{ \AA}$  and the flexible cable allowed measurement of spectral intensity with minimal disturbance to the medium. A description of the instrument is in the next section.

\* Timothy Quakenbush and Gerd Wendler, Geophysical Institute, University of Alaska, Fairbanks, Alaska 99775, U.S.A.  
Manuscript received 30 November 1993; accepted 5 April 1994.

## INSTRUMENTATION

The spectrometer used in this field study was a scanning Ebert-Fastie design with a 0.5 m focal length mirror. The instrument was manufactured by Fisher Scientific Company (FISHER SCIENTIFIC 1971). FASTIE (1952) originally described this arrangement of optics. The instrument uses a single grating with a groove spacing of 1180 grooves/mm. The entrance and exit slits are curved, 20 mm long, and the width can be adjusted from 5  $\mu\text{m}$  to 3 mm. A slit width of 50  $\mu\text{m}$  was used for our measurements, giving an optical bandwidth of about 0.2 nm at the detector.

The primary innovation of the spectrometer is the use of a quartz optical fiber light guide. Light is fed to the entrance slit through the light guide and a diffuser. Fig. 1 shows a drawing of the optics. The cable is 5 m long with a total cross section active area of 3.25 mm<sup>2</sup>. It is made of a bundle of 25  $\mu\text{m}$  core diameter synthetic quartz fibers. Both ends are terminated with stainless steel ferrules. The field of view of the cable end is 12°.

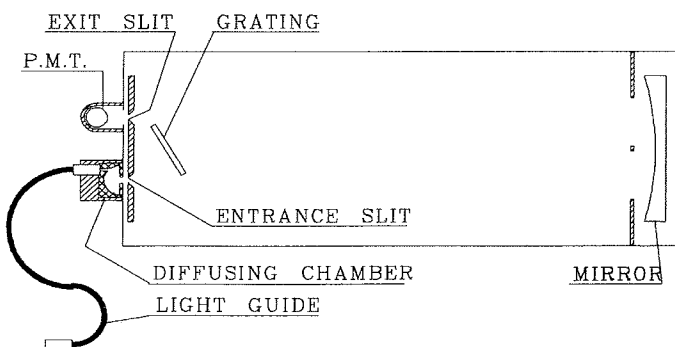


Fig. 1: Schematic of the spectrometer optics with synthetic quartz fiber optic light guide, entrance light diffuser, and photomultiplier tube (PMT) detector.

Abb. 1: Schematische Darstellung der Optik des Spektrometers.

The diffuser is necessary to uniformly illuminate the entrance slit with the non-uniform cone of light emitted from the cable. It is a 3 cm hemispheric cavity machined from Spectrolon, a very white reflective plastic. The open face of the hemisphere is covered by a Spectrolon mask that covers areas not in view of the entrance slit's narrow field of view. Light from the cable enters through a 3.5 mm hole in the side of the hemisphere and is diffusely reflected from the mask plate back into the chamber. The slit sees the diffusely illuminated area on the center of the hemisphere surface.

A system of optical encoders, grating drive motor, and a portable computer control and monitor the position of the grating which determines the wavelength of light that reaches the photomultiplier tube (PMT) detector. The wavelength scan rate is programmable from 0-550 nm/s with a tolerance of 1%. The computer tracks the wavelength of light entering the PMT over the range 200.00-900.00 nm with an accuracy of 0.01 nm.

The detector system is a 1P28 series photomultiplier tube and an electrometer. Its usable range is from 300-650 nm. The electrometer amplifies the nanoampere sized current from the PMT

to a measurable voltage. A sampling board in the computer converts the voltage to 12 bit numbers at a rate of 11 kHz. Sums and sample counts of the digitized electrometer voltage are stored in consecutive bins along with the wavelength of the end of the bin. The width of the bins can range from 0.01-655.35 nm/bin. The measurements presented here use a width of 1nm/bin.

Support instrumentation included a PD-1 Davos pyranometer and a Linke Feußner pyrliometer to verify constancy in the incoming radiation field during spectral sampling. Other meteorological and glaciological equipment were used as additional support.

## PLACE AND TIME OF OBSERVATIONS

The measurements were taken on the Juneau Icefield which lies north of Juneau, Alaska. There are about 4000 km<sup>2</sup> of glacierized terrain. The specific location was the Taku Glacier, one of the larger glaciers (18 km length) of the icefield. More than 40 years of glaciological work has been carried out on the Juneau Icefield under the leadership of M. Miller (e.g. MILLER 1957, BYERS et al. 1988, WENDLER & STRETEN 1969). Measurements were carried out on the Taku Glacier close to Camp 10 (58° 37' N, 134° 30' W, altitude of 1077 m), one of many research and training camps established by M. Miller. Our group occupied the camp from 21 July to 4 August 1991.

There had been a new snow fall on 18 July, but by the time measurements were able to begin three days later, the snow was melting. The snow grain size was 1.0-1.2 mm, and the density ranged from 0.50-0.55 g cm<sup>-3</sup>. Measurements were obtained under different sky conditions. For example, there were clear skies on 21 July, medium to thin stratus clouds on 26 July, and thick stratus with drizzle on 27 July 1991.

## OBSERVATIONS

### Downward Irradiance

The solid line in Fig. 2 shows a measured spectrum of direct beam solar irradiance between 330-600 nm. The measurement was taken at 10:45, 21 July 1993 Alaska local time under clear sky conditions. The data have been converted from PMT current to irradiance by comparison to a standard lamp. Since the cable end has a 12° field of view, the spectrum also includes light scattered in small forward angles. The major Fraunhofer solar absorption lines can easily be seen in the measured spectrum. A few are labeled in Figure 2.

The dotted line in Fig. 2 represents the spectrum of direct beam solar irradiance above the Earth's atmosphere taken from IQBAL (1983). The agreement between the two curves gives confidence in the instrumentation used. Not only are the general forms of the spectra similar, but the peaks also occur at the correct wavelength. Both curves are normalized to their respective irradiance value at 600 nm.

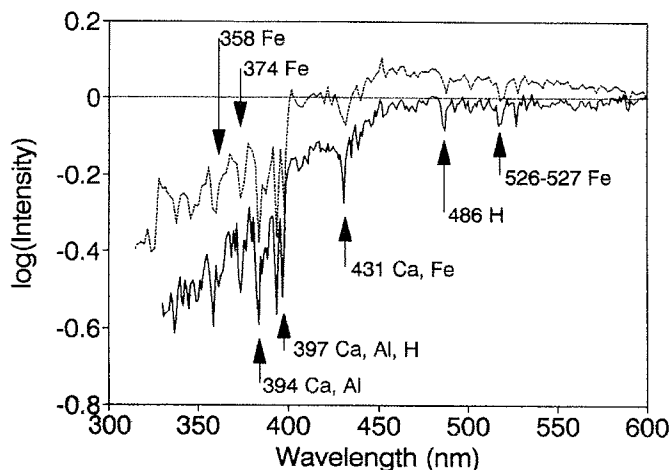


**Fig. 2:** The solid line is a direct beam spectral irradiance ( $F$ ) measured at 10:45, 21 July 1991 solar time (solar elevation =  $45^\circ$ ), on the Taku Glacier, Juneau Icefield, Alaska. The cable end was aimed at the sun under clear sky conditions. The dotted line is the direct beam spectral irradiance ( $F$ ) above the Earth's atmosphere as reported by IQBAL (1983). Each curve has been normalized to the irradiance at 600 nm ( $F_0$ ).

**Abb. 2:** Direkte Sonnenstrahlung ( $F$ ) als Funktion der Wellenlänge (durchgezogene Kurve) gemessen um 10.45 h Solarzeit am 21 Juli 1991 (Sonnenhöhe  $45^\circ$ ) unter wolkenlosen Bedingungen auf dem Taku Gletscher, Juneau Icefield, Alaska. Die gestrichelte Kurve gibt die gleichen Werte außerhalb der Atmosphäre nach IQBAL (1983). Beide Kurven wurden auf 600 nm ( $F_0$ ) normiert.

In Fig. 3 measurements of diffuse sky radiance under clear and cloudy (stratus clouds) sky conditions are presented. In both cases collected light was traveling straight down in the  $12^\circ$  field of view of the cable end. These curves are in units of current from the PMT detector ( $I$ ) in microamperes. As expected the spectral radiance for the clear sky is about an order of magnitude less than for the cloudy sky since water drops scatter light across the observed wavelengths, and air scatters according to Rayleigh scatter.

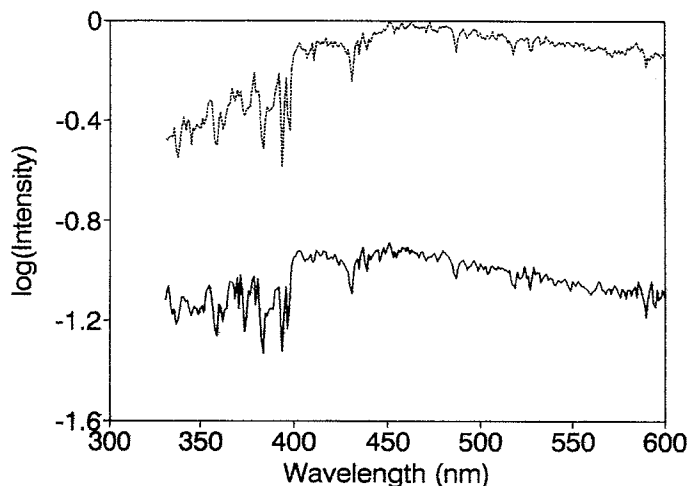


**Fig. 3:** Microamperes ( $I$ ) from the light detector for measurements of downward sky spectral radiance under clear (solid line) and cloudy (dotted line) conditions. The light was collected by pointing the optic cable end straight up ( $12^\circ$  field of view). The solar elevations were  $46^\circ$  and  $44^\circ$  respectively.

**Abb. 3:** Intensität ( $I$ ) der spektralen Strahlung im Zenith in Mikroampere für wolkenlose (durchgezogene Linie) und total bedeckte (gestrichelte Linie) Bedingungen. Der Öffnungswinkel des Instrumentes ist  $12^\circ$  und die Sonnenhöhen betragen  $46^\circ$  und  $44^\circ$ .

The scattering and absorption by stratus cloud cover can also be seen in Fig. 4. The solid line is the ratio of diffuse clear sky radiance to the direct beam. The dotted line is the ratio of the diffuse sky radiance measured under a thick stratus cloud layer to the direct beam. The same direct beam spectral radiance is used for both ratios. Both curves are normalized at 450 nm. The solid curve shows that a cloud free atmosphere scatters light into the optic cable's field of view much more strongly toward shorter wavelengths, as expected from Rayleigh scattering. Measurements of diffuse to direct ratios by GARRISON et al. (1978) display an increase farther into the UV. Photographs with a 320 nm filter taken by LIVINGSTON (1983) reveal a bright, optically thick atmosphere.

The dotted curve has a flat maximum from about 450-550 nm, and drops off toward the UV and yellow-red. This is consistent with the solar beam being scattered by a water cloud with drop sizes much larger than the wavelength of observed light. Large drop size means even scattering across the wavelength range, and water absorbs more in the UV and yellow-red compared to the blue and green region.

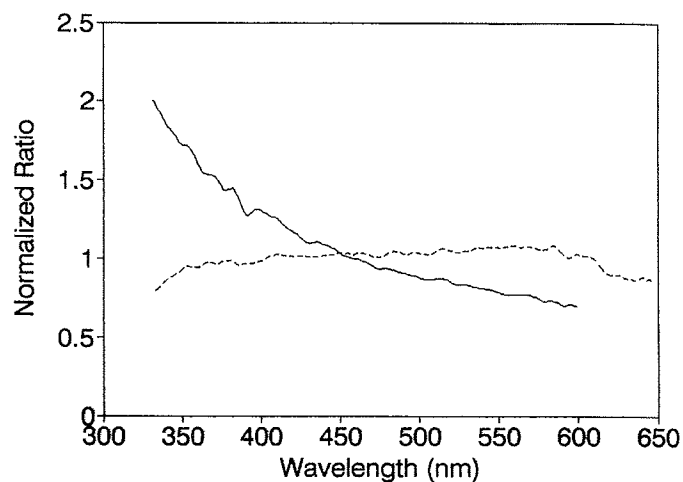


**Fig. 4:** Downward spectral radiance ratios. The solid line is the clear sky diffuse radiance divided by the clear sky direct beam. The dotted line is the downward diffuse radiance measured under a thick stratus cloud layer divided by the same direct beam measurement. Both curves are normalized at 450 nm. The clear sky and direct solar beam measurements were taken near 11:00, 21 July 1991 solar time (solar elevations =  $46^\circ$  and  $44^\circ$  respectively), and the cloudy sky measurement was taken at 10:44, 27 July 1991 solar time (solar elevation =  $43^\circ$ ). The sky radiance measurements were taken by pointing the optic cable end straight up ( $12^\circ$  field of view).

**Abb. 4:** Verhältnis der diffusen und direkten Sonnenstrahlung unter wolkenlosen Bedingungen (durchgezogene Kurve) und Verhältnis der diffusen Strahlung unter einer dicken Stratus-Wolkendecke zur direkten Strahlung unter wolkenlosem Himmel (gestrichelte Linie). Beide Kurven wurden auf 450 nm normiert und der Öffnungswinkel betrug für alle Messungen  $12^\circ$ . Die Messungen wurden am späten Vormittag des 21. Juli 1991 (wolkenlos) und am 27. Juli 1991 (total bedeckt) ausgeführt. Die diffuse Strahlungsmessungen wurden im Zenith gemacht.

#### Albedo

The terms reflectivity and albedo have different meaning in this article. Reflectivity is the upward traveling radiance reflected from a surface, divided by the downward traveling radiance

from the sky. The measured radiance values are monochromatic, and contain light collected in the  $12^\circ$  field of view of the optic cable end. Albedo refers to the spectrally integrated irradiance reflected from a surface, divided by the integrated downward sky irradiance. The irradiance values measured here were done with the Davos pyranometer which collects light in a  $2\pi$  solid angle.

Snow has the highest reflectivity of all natural substances. Albedo values in excess of 90 % have been observed for new dry snow. The albedo is not only high but also can vary widely depending on snow age, grain size, and contaminants (e.g. BOLSENGA 1983). Pioneering work was carried out by LILJEQUIST (1954) in Antarctica, and by DIRMHIRN & TROJER (1955) in the Austrian Alps.

A fairly complete model of the optical properties of snow from the visible to infrared with and without contaminants were produced by WARREN (1982). The reflectivity was found to depend strongly on snow grain size, snow age, contaminate concentration, and whether the snow had never melted, was wet, or refrozen.

Reflectivity was calculated from two spectral measurements. It is the ratio of the upward traveling radiance reflected from the snow surface divided by the downward sky radiance. The radiance values were measured by directing the  $12^\circ$  field of view of the optic cable end straight up at the sky, and straight down at the snow surface. The measurements were made under a thick stratus cloud layer to ensure isotropic sky radiance so that the reflectivity can be comparable to measurements with the  $2\pi$  pyranometer measurements. The spectral reflectivity (solid line in Fig. 5) shows a fairly strong dependence on wavelength. It has its maximum in the blue-green, and drops in the UV and yellow-red wavelength bands. For comparison, the dotted line in Fig. 5 is from measurements in the visible range by GRENFELL & MAYKUT (1977), carried out on snow covered ice near the T-3 ice island in the Arctic Ocean; the shorter dashed line is from model calculations by WARREN (1982) for 1 mm snow grains with a volcanic ash concentration of 10 ppm by weight and the longer dashed line is for alpine snow from GRENFELL & PEROVICH (1982). All reflectivity curves agree between 400-600 nm except for the GRENFELL & PEROVICH (1982) data. Our measurements give a lower reflectivity toward the UV, which is more in agreement with previously published results by DIRMHIRN (1967) and EATON & DIRMHIRN (1979). This is furthermore in agreement with results published by AMBACH & EISNER (1986), who compared UV to the global radiation. They found similar results to ours for „dirty“ snow, but the opposite for clean one. This effect is likely due to multiple reflection between the snow surface and cloud layer (WENDLER et al. 1981), since both absorb more in the UV and yellow-red ranges than in blue or green. A model by DOZIER et al. (1989) shows similar values to those presented in Fig. 5.

The mean reflectivity for our measured range of 350-600 nm was 87 % for the snow on the Taku Glacier. The integrated albedo over the entire spectrum was measured by the Davos pyra-

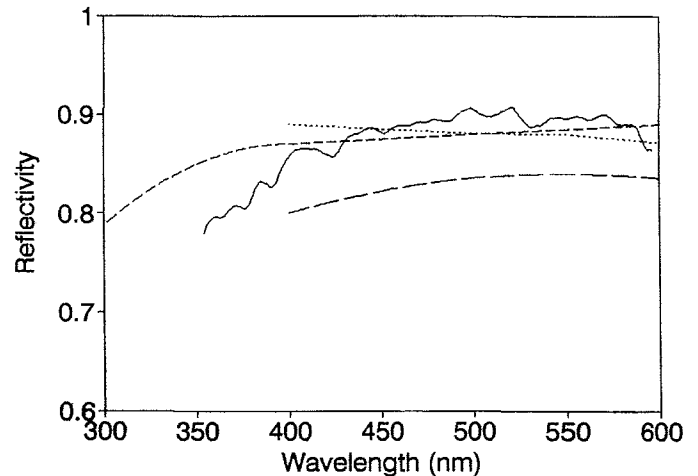


**Fig. 5:** The solid line is the spectral reflectivity of snow taken on the Taku Glacier, 27 July 1991. Note that the reflectivity has its maximum in the blue-green, and decreases both for longer and shorter wavelength. The dotted line is a measured spectrum by GRENFELL & MAYKUT (1977) carried out near T-3 in the Arctic Ocean, the shorter dashed line is from model calculations by WARREN (1982) for snow with a volcanic ash concentration of 10 ppm by weight, and the long dashed line is alpine snow from GRENFELL & PEROVICH (1981).

**Abb. 5:** Spektrale Reflexion des Schnees auf dem Taku Gletscher am 27 Juli 1991 (durchgezogene Kurve). Die Reflexion hat ihr Maximum im blaugrünen, und nimmt sowohl für längere als auch für kürzere Wellenlängen ab. Die punktierte Kurve repräsentiert Werte von T-3 (Polarmeer) nach GRENFELL & MAYKUT (1977), die kurz-gestrichelte Kurve Modellwerte nach WARREN (1982) für Schnee mit einer Verschmutzung mit Vulkanasche von 10 ppm. Die langgestrichelte Kurve beruht auf Messungen alpinen Schnees nach GRENFELL & PEROVICH (1982).

nometer at 66 %. The difference is expected since the pyranometer includes the red and near IR. The reflectivity of wet snow in these regions is substantially lower.

For comparison, the mean reflectivity was estimated from the model calculations used for the short dashed line in Figure 5 (WARREN 1982). The mean is about 87 % in the 300-600 nm band, 33 % in the 600-1500 nm band, and 55 % for the full range of 300-1500 nm.

#### Light Extinction

Measurement of spectral extinction in a snow pack has been difficult in the past (AMBACH & MOCKER 1959). It has been common to place a filter radiometer in an undercut hole, or at the end of a snow column. These methods lead to considerable disturbance of the snow-pack which can lead to significant errors. Another method is to take snow or ice samples to a laboratory and analyze them using an artificial light source. Again, many errors are encountered (WENDLER 1970).

The use of a fiber optic cable greatly reduces the snow-pack disturbance. A 1 m wide by 1.5 m deep trench was dug in the snow pack to carry out our measurements. Horizontal holes were drilled in the walls of the trench at several depths. The holes were 1 m long with a diameter of 2 cm. The end of the cable was then inserted into the holes. The collected light was travel-

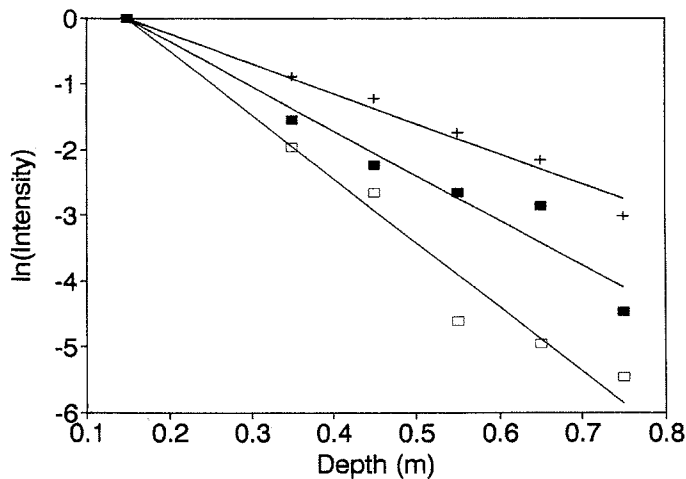


**Fig. 6:** The natural log of the light detector current for measurements of radiance in different wavelength bands vs. snow depth. For totally uniform snow, a straight line is expected. The symbols are: Filled square = 350-370 nm, plus = 450-470 nm, and empty square = 590-610 nm. The 590-610 nm (red) band shows the strongest decrease with depth, while 450-470 nm (blue) is absorbed the least. 350-370 nm (UV) lies between these two values. The 520-540 nm band (green, which is not shown) displayed very similar values to the UV.

**Abb. 6:** Natürlicher Logarithmus der Lichtintensität aufgetragen gegen die Schneetiefe für verschiedene Wellenlängenbereiche. Für eine gleichförmigen Schneedecke ist eine Gerade zu erwarten. Gefüllte Quadrate = 350-370 nm, Plus-Zeichen = 450-470 nm, nicht gefüllte Quadrate = 590-610 nm. Die Intensitätsabnahme mit der Tiefe von rotem Licht (590-610 nm) ist am stärksten, die des blauen Lichts am schwächsten. Für ultraviolettes Licht (350-370 nm) liegt die Abnahme zwischen den beiden Werten. Grünes Licht (520-540 nm) - in der Abbildung nicht gezeigt - zeigte ähnliche Werte wie ultraviolettes Licht.

ing horizontally within the 12° field of view of the cable end. The same technique was used by GRENFELL & MAYKUT (1977) to measure extinction in the visible region. The assumption that below the surface layer, snow scatters light strongly enough to make the horizontally directed radiance proportional to the downward irradiance is used to calculate extinction.

In Figure 6 the natural log of horizontal radiance ( $I$ ) in three integrated wavelength bands is plotted against depth. A linear regression is drawn for each band. For totally uniform snow, a straight line is expected according to the Bouguer-Lambert Law. The point scatter around each line in Figure 6 is expected because the snow pack is not uniform. Extinction coefficients ( $k$ ) are found from the linear regression lines. The red (590-610 nm) shows the strongest decrease with depth ( $k = 9.8 \text{ m}^{-1}$ ), while in the blue (450-470 nm) the absorption is at a minimum ( $k = 4.6 \text{ m}^{-1}$ ). The ultraviolet (350-370 nm) lies between these two values ( $k = 6.8 \text{ m}^{-1}$ ). Green (520-540 nm), which is not shown in the graph, displayed a very similar values to the UV ( $k = 6.7 \text{ m}^{-1}$ ).

The extinction coefficient as a function of wavelength is given in Figure 7. The lowest values of  $4.2 \text{ m}^{-1}$  were found near 480 nm, while the highest values of  $8.8$  and  $7.5 \text{ m}^{-1}$  occurred at 350 and 580 nm, respectively. The extinction curve explains why the walls of a snow or ice cave look blue, where there is a minimum

in spectral extinction. Extinction coefficient model calculations by WARREN (1982) for pure snow with a crystal size of 1.3 mm are also included in Figure 7. The shape of the two curves is very similar.

## CONCLUSION

The use of a quartz fiber optic bundle greatly aids light extinction measurements. It makes intensity measurements possible with only a small disturbance to the medium in question. Spectral sky and reflectivity measurements are simplified by orienting the cable end instead of the entire spectrometer.

A comparison of spectral intensities for clear and cloudy conditions shows all wavelengths being strongly scattered by clouds. The cloud layer was optically thicker in the UV-A and yellow-red compared to the blue-green band.

Reflectivity and extinction measurements agree generally with previous work, both actual observations and model calculations. The maximum in reflectivity and the minimum in extinction were measured at a wavelength of 480 nm (blue). Towards the UV, and even to a greater extent towards the longer wavelengths the reflectivity decreased and the extinction coefficient increased.

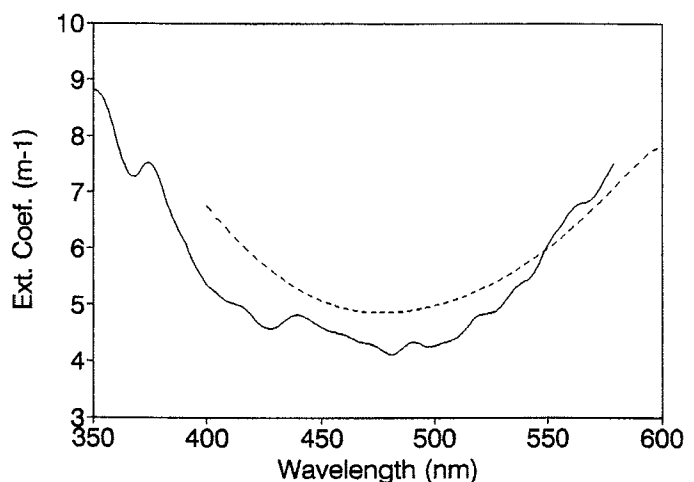


**Fig. 7:** The solid curve is the extinction coefficient in snow on Taku Glacier, 26 July 1991. The dotted curve is from model calculations for pure snow with a snow grain size of 1.3 mm (WARREN 1982)

**Abb. 7:** Extinktionskoeffizient des Schnees auf dem Taku Gletscher am 26. Juli 1991 (durchgezogene Linie). Die punktierte Kurve repräsentiert Werte nach Modellberechnungen für eine Kristallgröße von 1,3 mm nach WARREN (1982).

## ACKNOWLEDGMENT

This study was supported by NSF Grant, DPP 90-17969. Dr. Maynard M. Miller, Director, Juneau Icefield Research Program under the aegis of the Foundation for Glacier and Environmental Research supported us generously. Further, the help of Carl Byers and the student intern Andrew Otto it gratefully acknowledged.

## References

- Ambach, W. & Eisner, H.* (1986): Albedo verschiedener Schneeoberflächen für enrytherm wirksame solare Strahlung.- *Wetter und Leben* 38: 1-4.
- Ambach, W. & Mocker, H.* (1959): Messungen der Strahlungsextinktion mittels eines kugelförmigen Empfängers in der oberflächennahen Eisschicht eines Gletschers und im Alteis.- *Archiv Meteorol. Geophys. Bioklimatol. B*, 10: 84-99.
- Bolsenga, J. S.* (1983): Spectral Reflectance of Snow and Fresh-Water Ice from 340 through 1100 nm.- *Jour. Glaciol.* 29: 296-305.
- Brune, W. H.* (1991): Stratospheric Chemistry.- *Rev. Geophys., Suppl.*: 12-24.
- Byers, C., Daellenbach, K., Markillie, J., McGee, S. & Peterson, E.* (1988): Results of the Summer 1988 Surveying Program.- *Rep. Juneau Icefield Research Program*, pp. 45.
- Crutzen, P. & Arnold, F.* (1986): Nitric Acid Cloud Formation in the Cold Antarctic Atmosphere: a Major Cause for the Springtime „Ozone Hole“.- *Nature* 324: 651-655.
- Dirmhirn, I. & Trojer, E.* (1955): Albedomessungen auf dem Hintereisferner.- *Archiv Meteorol. Geophys. Bioklimatol. B*, 6: 400-416.
- Dirmhirn, I. & Eaton, F.* (1975): Some Characteristics of the Albedo of Snow.- *Jour. Applied Meteorol.* 14: 375-379.
- Dozier, J., Davis, R. & Nolin, A.* (1989): Reflectance and Transmittance of Snow at High Spectral Resolution.- *IEEE Geosci. Remote Sensing Soc.* 2: 662-664.
- Eaton, F. & Dirmhirn, I.* (1979): Reflected Irradiance Indicatrices of Natural Surfaces and their Affect on Albedo.- *Applied Optics* 18: 994-1008.
- Farman, J., Gardiner, B. & Shanklin, J.* (1985): Large Losses of Total Ozone in Antarctica Reveal Seasonal ClOx/NOx Interaction.- *Nature* 315: 207-210.
- Fastie, W.* (1952): A small Plane Grating Monochromator.- *Jour. Optical Soc. Amer.* 42: 641-647.
- Fisher Scientific Co.* (1971): Instruction Manual for the 82-000 Series 0.5 m Ebert Scanning Spectrometer.- *Engineering Publ. No. 82-000/IM Rev 7.*
- Garrison, L., Murray, I., Doda, D. & Green, A.* (1978): Diffuse-Direct Ultraviolet Ratios with a Compact Double Monochromator.- *Applied Optics* 17: 827-836.
- Grenfell, T. & Perovich, D.* (1981): Spectral Albedos of an Alpine Snow Pack.- *Cold Regions Sci. Technol.* 4: 121-127.
- Iqbal, M.* (1983): *An Introduction to Solar Radiation.*- pp. 390, Academic Press.
- Liljequist, G. H.* (1954): Radiation and Wind and Temperature Profiles over an Antarctic Snowfield.- *Toronto Meteorol. Conf., Royal Meteorol. Soc. London*, 78-87.
- Livingston, W.* (1983): Landscape as viewed in the 320 nm Ultraviolet.- *Jour. Optical Soc. Amer.* 37: 1653-1657.
- Miller, M.* (1957): Phenomena Associated with the Deformation of a Glacier Bore-Hole.- *Extrait Comt. Rapp., Assembl. Gen. Toronto*, 440-441.
- Warren, S.* (1982): Optical Properties of Snow.- *Rev. Geophys. Space Phys.* 20: 67-89.
- Wendler, G.* (1970): Some Measurements of the Extinction Coefficient of River Ice.- *Polarforschung* 6: 253-256.
- Wendler, G., Eaton, F. & Ohtake, T.* (1981): Multiple reflection effects on Irradiance in the Presence of Arctic Stratus Clouds.- *Jour. Geophys. Res.* 86: 2049-2057.
- Wendler, G. & Streten, N.* (1969): Short Term Heat Balance Study on a Coast Range Glacier.- *Pure Appl. Geophys.* 77: 68-77.